Supplement of Biogeosciences, 23, 3675–3695, 2026
https://doi.org/10.5194/bg-23-3675-2026-supplement

Biogeosciences Open Access EGU

Supplement of

Sedimentary insights into organic matter alteration in Arctic Alaska's saline permafrost

Fabian Seemann et al.

Correspondence to: Fabian Seemann (fabian.seemann@awi.de)

Table S1: Characteristics of coring sites on the Utqiaġvik Peninsula.

	Upland	West Twin Lake	East Twin Lake	DLB	Thermokarst lagoon	Elson lagoon
Coring date	2022.04.21	2022.04.19	2022.04.20	2022.04.22	2022.04.20	2022.04.21
Latitude	71.27637	71.27396	71.2753	71.2772	71.2632	71.29008212
Longitude	-156.45296	-156.49699	-156.45296	-156.44311	-156.42355	-156.47186
Elevation (m a.s.l.)	3.3	2.0	2.4	2.9	0.0	0.0
Area (km^2)	n/a	1.306	1.276	1.051	0.801	125
Sediment core length (cm)	204	23	259	142	46	110
Total sample number	34	4	26	26	10	21
Sediment physical state	frozen	unfrozen	unfrozen	frozen	unfrozen	semi-frozen
Coring device	SIPRE	Push	Vibra	SIPRE	SIPRE	SIPRE
Waterbody depth (cm)	n/a	181	175	n/a	94	116
Ice thickness (cm)	n/a	175	146	n/a	94	116
Total water depth (cm)	n/a	181	175	n/a	94	116
Liquid water temperature (°C)	n/a	0.04	0.30	n/a	-12.7	-
Liquid water electrical conductivity ($mS\ cm^{-1}$)	n/a	0.002	12.0	n/a	20.2	-

Table S2: Upland core photograph and description (picture: Fabian Seemann). In the top-left of the photograph, the top of the core is visible, and in the bottom-right the core bottom is located. The core is split in halves and cleaned in a climate chamber to reveal colors, structures and properties.

Photograph	Depth (cm)	Description
	0-3	Recent vegetation, dark brown.
	3-12	Light brown layers, ice lenses of 1 cm length between 4-8 cm, massive ice between 8-12 cm, silty, peat band of 2 cm diameter at 7 cm depth.
	12-38	Ice-rich, dark/light brown cryoturbated, organic-rich, few macro plant remains at 27 cm, silty peat.
	38-69	Silty light grey, ataxitic, macro plant remains.
	69-83	ice-rich, dark brown, organic-rich, cryoturbation at 77-82 cm.
	83-133	Light-grey silty, no organic remains visible, very ice-rich, reticular ice lenses.
	133-174	Grey (darker than above), silty, reticula and lenticula ice lenses, ice bands.
	174-193	Darker than above, very ice-rich (50 %), silty, thick lenses (1 cm chaotically orientated), no orgacnics visible.
	193-204	Ataxitic with sediment inclusions.

Table S3: West Twin Lake core photograph and description (picture: Fabian Seemann).

Photograph	Depth (cm)	Description
	0-23	Blackish brown, poorly decomposed organic matter, no minerals visible, drier downwards.

Table S4: East Twin Lake core photograph and description (pictures: Fabian Seemann). The core is compressed by 118 cm due to vibration during coring.

Photograph	Depth (cm)	Description
	0-15	Dark brown, macro-remains, poorly decomposed, high water content, no minerals visible.
	15-22	Lighter brown to grey-ish, fine minerals, poorly decomposed organics, macro-remains.
	22-27	Black/brown (organics), grey-blue-ish (minerals).
	27-51	High water content, fine sand, silty, yellow-ish, grey, few macro remains.
	51-60	As above but more oxidized, more orange, lower water content, woody macro remains at 59 cm.
	60-80	Black-ish, dark grey to medium grey, less water content, no plant macro remains, visible fines (clayey silt).
	80-93	Dark grey-ish, black, coarser as above, oxidized, organic inclusions (brown grey).
	93-108	Continuation of brownish-grey silty material.
	108-128	Dark, blackish-grey, silty and denser.
	128-138	Same color but less dense, more water due to higher pore space.

Table S5: Drained Lake Basin core photograph and description (pictures: Fabian Seemann).

Photograph	Depth (cm)	Description
	0-14	Water saturated peat, 8-14 cm partly decomposed peat, black/brown.
	14-18	Less water saturated, more peat than water, first sediment inclusions.
	18-21	Transition peat to silt, brown grey, diagonal macro-lense (3*0.5 cm horizontal wavy micro-lenses).
	21-29	Brown grey, silt, horizontal macro-lense 1*0,5 cm, two large vertical cracks (6 cm long, 0.5 cm wide).
	29-33	Pure peat (sec. Lake phase prob.), brown to light brown.
	33-79	Ich-rich, lenticula (max. 0.5 cm thick), also reticula structure, at 39 cm (1*1 cm) organic inclusion, at 45-52 cm and 62-71 thicker ice lense.
	79-93	Cryoturbated horizon, black-brown (org.)-grey (sandy silt) turbations, 90-93 cm black band, thin ice-lenses 1 mm, 3 cm long.
	93-97	Sandy-silt band, ice band 1 mm horizontal 5 cm long, more smaller ice bands vertical + horizontal, at 96-97 cm black circular structure (1 cm diameter).
	97-104	Brown matrix with macro remains, sandy silt, mixed with black (highly decomposed) fine silts.
	104-107	Sandy silt, grey, macro remains, few micro-lenses.
	107-115	Dark black, highly decomposed.
	115-122	Brown grey, sandy silt, black dots of 0.5 cm, structureless.
	122-131	As above, less black, ice-rich along the core-side.
	131-142	Sandy silt, with micro-lenses (horizontal, few vertical), like above concerning ice content.

Table S6: Semi-open thermokarst lagoon core photograph and description (pictures: Fabian Seemann).

Photograph	Depth (cm)	Description
	0-2	Grey, brown, fines.
	2-9	Black, loose organics, ice-bands without orientation 1 mm.
	9-11	Brown grey, fines, organic-rich, vertical ice-bands 1 mm.
	11-12	Grey, silt band.
	12-23	Like at 2-9 cm, fine laminated, black, organic-rich.
	23-31	Laminated with wider (4-5 mm), vertical ice-bands, greyish black.
	31-40	Laminated, wider than above, no ice-bands.
	40-43	Black, brown, laminated.
	43-46	Black dots, not laminated.

Table S7: Elson Lagoon core photograph and description (pictures: Fabian Seemann).

Photograph	Depth (cm)	
	0-6	Dark brown, fine laminated, un-orientated 2 mm ice-bands.
	6-9	3-4 mm thick ice-bands, un-orientated, more ice than above, brown.
	9-16	Unfrozen structureless, dark brown.
	16-27	Horizontal laminations, 3-4mm, black, brown, grey, silty; at 16-24 cm horizontal ice bands 1 mm thick, at 24-27 cm un-orientated ice-bands.
	27-31	3 laminations: light brown, grey.
	31-36	Horizontal ice-bands 2-4 mm wide.
	36-37	Finer than above, thin horizontal ice-bands.
	37-44	Horizontal ice-bands, laminated, coarser than above, silty.
	44-63	Un-orientated ice-bands 1-3 mm wide, light brown grey, laminations.
	63-65	Very fine laminations, brighter downwards, fine vertical ice-bands.
	65-66	Like at 44-63 cm but darker.
	66-78	Ice-bands 1 mm wide from vertical to horizontal (cryoturbated?), dark dots in bright silt.
	78-93	Laminations dark black, brown, sand (at 79 cm, 84 cm) microlenses vertical and horizontal (potentially through deformation).
	93-98	Sandy silt to silty sand transition, brownish grey, lighter than above.
	98-101	Sand layer, 3 rounded pebbles (diameter 2 cm), 1 pebble of granite (?).
	101-110	Sediment layers of 0.5 cm brown, grey, black, slightly; u-shaped (deformation by corer?), silty sand, sandy silt.

Table S8: Radiocarbon data.

AWI MICADAS sample ID*	Sample label	Depth (cm)	Material dated	^{14}C age (yr BP)	+/-	Calibrated age 2s range (yr cal BP)**	Mean calibrated age (yr cal BP)
12524.1.1	BRW22-UL 5-14	7.5	Plant remains	-157	54		modern
12525.1.1	BRW22-UL 25-30	27.5	Plant remains	5,734	69	6,392-6,675	6,534
12526.1.1	BRW22-UL 50-55	52.5	Plant remains	5,931	72	6,604-6,946	6,775
12527.1.1	BRW22-UL 70-80	75	Plant remains	6,105	73	6,785-7,165	6,975
12528.1.1	BRW22-UL 98-106	102	Plant remains	6,074	76	6,777-7,159	6,968
12529.1.1	BRW22-UL 123-128	125.5	Plant remains	6,394	77	7,161-7,430	7,296
12530.1.1	BRW22-UL 180-192	186	Bulk sediment	11,413	32	13,179-13,347	13,263
12520.1.1	BRW22-WTL 3-13	8	Plant remains	2,285	60	2,121-2,432	2,277
12521.1.1	BRW22-ETL 3-13	8***	Plant remains	2,810	64	2,765-3,075	2,920
12522.1.1	BRW22-ETL 70-80	75***	Bulk sediment	23,542	60	27,596-27,863	27,730
12523.1.1	BRW22-ETL 116-126	121***	Bulk sediment	38,823	194	42,371-42,761	42,566
12531.1.1	BRW22-DLB 19-22	20.5	Plant remains	709	57	623-729	676
12532.1.1	BRW22-DLB 26-35	30.5	Plant remains	1,311	30	1,242-1,294	1,268
12533.1.1	BRW22-DLB 50-55	52.5	Plant remains	2,129	107	1,865-2,342	2,104
12534.1.1	BRW22-DLB 70-77	73.5	Plant remains	9,348	87	10,255-10,768	10,512
12535.1.1	BRW22-DLB 105-110	107.5	Plant remains	8,842	36	9,723-9,968	9,846
12536.1.1	BRW22-DLB 131-142	136.5	Bulk sediment	29,541	87	33,877-34,376	34,127
12540.1.1	BRW22-SOL 16-21	18.5	Plant remains	6,369	142	6,949-7,514	7,232
12541.1.1	BRW22-SOL 41-46	43.5	Plant remains	4,096	114	4,290-4,860	4,575

12537.1.1	BRW22-EL 0-4	2	Plant remains	4,811	111	5,308-5,753	5,531
12538.1.1	BRW22-EL 34-39	36.5	Plant remains	4,694	114	5,046-5,605	5,326
12539.1.1	BRW22-EL 74-78	76	Plant remains	5,312	84	5,929-6,224	6,077

* AWI MICADAS sample number based on Mollenhauer et al.(2021).

** Radiocarbon calibration was conducted using Calib 8.20 software and the IntCal 20 calibration curve (Reimer et al., 2020; Stuiver and Reimer, 1993).

***East Twin Lake core 118 cm compressed

Table S9: Summary statistics and Kruskal-Wallis test results for geochemical parameters across thermal regimes. Sample count (n) in individual groups with reduced number after n/a removal in brackets (only samples with complete TOC, C:N, and $\delta^{13}C$ data were tested). *Seasonally frozen* is composed of upland (n = 8) and DLB (n = 9) samples, perennially *frozen* of upland samples, and *unfrozen* of West (n = 4, effectively 3) and East Twin Lake (n = 26, effectively 6) samples. *Refrozen* samples represent DLB samples, and *lagoon* samples are from the semi-open thermokarst lagoon (n = 10, effectively 9) and Elson Lagoon (n = 21, effectively 17). Data are presented as mean ± SD (standard deviation) and median ± IQR (interquartile range). Kruskal-Wallis test statistics: χ^2 = chi-squared statistic, df = degrees of freedom, p = probability value. ε^2 (epsilon-squared) is the effect size measure for non-parametric tests, interpreted as: <0.01 = negligible, 0.01-0.04 = small, 0.04-0.16 = medium, 0.16-0.36 = large, >0.36 = very large effect.

Thermal regime	**n**	**TOC (wt%)**		**C:N ratio**		**$\delta^{13}C$ (‰ vs. VPDB)**	
		Mean (SD)	Median (IQR)	Mean (SD)	Median (IQR)	Mean (SD)	Median (IQR)
Seasonally frozen	17	18.7 (±13.2)	16.6 (14.3)	20.5 (±4.6)	20.0 (4.6)	-27.6 (±1.1)	-27.8 (1.7)
Frozen	26	10.7 (±5.6)	7.3 (7.6)	16.1 (±2.4)	14.8 (4.1)	-27.7 (±0.5)	-27.8 (0.6)
Unfrozen	30 (9)	4.7 (±5.9)	1.6 (5.1)	12.6 (±6.6)	16.9 (13.1)	-26.7 (±1.3)	-25.9 (2.4)
Refrozen	17	6.5 (±8.0)	2.7 (5.2)	17.4 (±4.2)	16.0 (3.7)	-27.3 (±0.9)	-27.4 (1.2)
Lagoon	31 (26)	4.9 (±1.9)	5.1 (2.1)	17.5 (±1.4)	17.6 (2.3)	-27.4 (±0.7)	-27.6 (0.2)
Kruskal Wallis		$\chi^2 = 46.9$, df = 4, $p = 1.62\times10^{-9}$, $\varepsilon^2 = 0.391$		$\chi^2 = 20.8$, df = 4, $p = 0.00034$, $\varepsilon^2 = 0.173$		$\chi^2 = 12.1$, df = 4, $p = 0.017$, $\varepsilon^2 = 0.100$	

Table S10: Summary statistics and Kruskal-Wallis test results for geochemical parameters across salinity classes. Sample count (n) in individual groups with reduced number after n/a removal in brackets (only samples with complete TOC, C:N, and $\delta^{13}C$ data were tested). *Freshwater* (< 1.5 mS cm^{-1}) is composed of upland (n = 24) and DLB (n = 3) samples. *Brackish* (1.5-15 mS cm^{-1}) includes upland (n = 9), West Twin Lake (n = 4, effectively 3), Est Twin Lake (n = 2), and DLB (n = 19) samples. *Saline* (15-50 mS cm^{-1}) comprises upland (n = 1), East Twin Lake (n = 24, effectively 4) and DLB (n = 4) samples. *Hypersaline* (>50 mS cm^{-1}) samples comprise semi-open thermokarst lagoon (n = 10, effectively 9) and Elson Lagoon (n = 21, effectively 17) porewaters. Data are presented as mean ± SD (standard deviation) and median ± IQR (interquartile range). Kruskal-Wallis test statistics: χ^2 = chi-squared statistic, df = degrees of freedom, p = probability value. ε^2 (epsilon-squared) is the effect size measure for non-parametric tests, interpreted as: <0.01 = negligible, 0.01-0.04 = small, 0.04-0.16 = medium, 0.16-0.36 = large, >0.36 = very large effect.

Salinity class	**n**	**TOC (wt%)**		**C:N ratio**		**$\delta^{13}C$ (‰ vs. VPDB)**	
		Mean (SD)	Median (IQR)	Mean (SD)	Median (IQR)	Mean (SD)	Median (IQR)
Freshwater	27	15.5 (± 9.2)	16.2 (12.5)	18.4 (± 3.1)	18.6 (5.1)	-27.5 (± 0.8)	-27.6 (1.3)
Brackish	34 (33)	10.8 (± 9.5)	7.4 (9.3)	17.7 (± 4.4)	16.9 (4.1)	-27.9 (± 0.7)	-28.0 (1.0)
Saline	29 (9)	2.1 (± 1.9)	1.6 (0.7)	10.4 (± 5.0)	12.7 (9.2)	-26.3 (± 0.9)	-25.8 (0.8)
Hypersaline	31 (26)	4.9 (± 1.9)	5.1 (2.1)	17.5 (± 1.4)	17.6 (2.3)	-27.4 (± 0.7)	-27.6 (0.2)
Kruskal Wallis		$\chi^2 = 68.33$, df = 3, $p = 9.74\times10^{-15}$, $\varepsilon^2 = 0.569$		$\chi^2 = 23.25$, df = 3, $p = 3.57\times10^{-5}$, $\varepsilon^2 = 0.194$		$\chi^2 = 40.40$, df = 3, $p = 8.77\times10^{-9}$, $\varepsilon^2 = 0.337$	

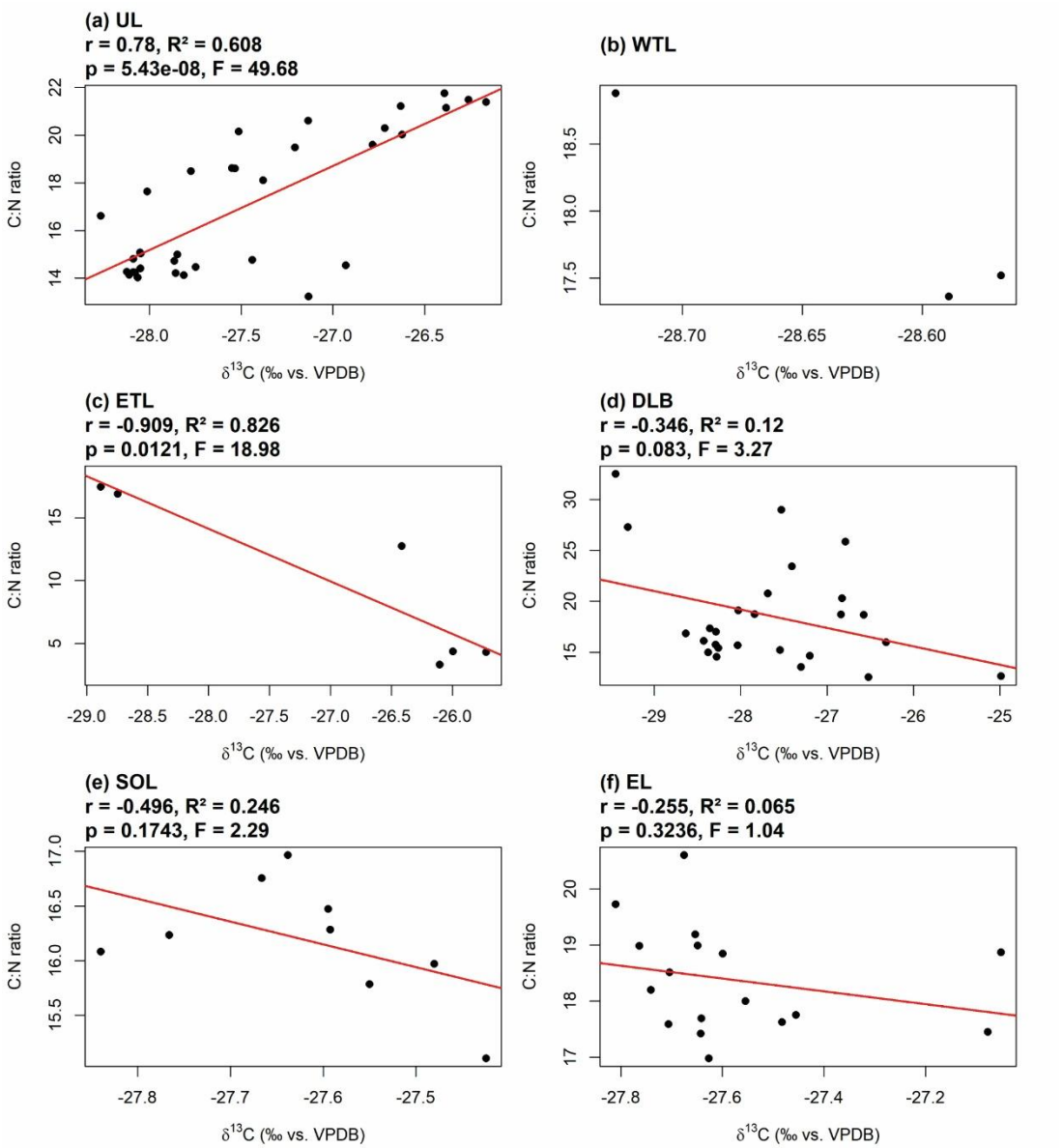

Figure S1: Correlation plots between C:N ratio and $\delta^{13}C$ (‰ vs. VPDB) for the different study sites: (a) UL (upland), (b) WTL (West Twin Lake), (c) ETL (East Twin Lake), (d) DLB (drained lake basin), (e) SOL (semi-open thermokarst lagoon), and (f) EL (Elson Lagoon).

References

Mollenhauer, G., Grotheer, H., Gentz, T., Bonk, E., and Hefter, J.: Standard operation procedures and performance of the MICADAS radiocarbon laboratory at Alfred Wegener Institute (AWI), Germany, Nuclear Instruments and Methods in Physics Research Section B: Beam Interactions with Materials and Atoms, 496, 45–51, https://doi.org/10.1016/j.nimb.2021.03.016, 2021.

Reimer, P. J., Austin, W. E. N., Bard, E., Bayliss, A., Blackwell, P. G., Ramsey, C. B., Butzin, M., Cheng, H., Edwards, R. L., Friedrich, M., Grootes, P. M., Guilderson, T. P., Hajdas, I., Heaton, T. J., Hogg, A. G., Hughen, K. A., Kromer, B., Manning, S. W., Muscheler, R., Palmer, J. G., Pearson, C., Plicht, J. van der, Reimer, R. W., Richards, D. A., Scott, E. M., Southon, J. R., Turney, C. S. M., Wacker, L., Adolphi, F., Büntgen, U., Capano, M., Fahrni, S. M., Fogtmann-Schulz, A., Friedrich, R., Köhler, P., Kudsk, S., Miyake, F., Olsen, J., Reinig, F., Sakamoto, M., Sookdeo, A., and Talamo, S.: The IntCal20 Northern Hemisphere Radiocarbon Age Calibration Curve (0–55 cal kBP), Radiocarbon, 62, 725–757, https://doi.org/10.1017/RDC.2020.41, 2020.

Stuiver, M. and Reimer, P. J.: Extended 14C Data Base and Revised CALIB 3.0 14C Age Calibration Program, Radiocarbon, 35, 215–230, https://doi.org/10.1017/S0033822200013904, 1993.